ELSEVIER

Chemistry & Biology 8 (2001) 1081–1094

Chemistry & Biology

www.elsevier.com/locate/chembiol

Research Paper

Peptides that mimic glycosaminoglycans: high-affinity ligands for a hyaluronan binding domain

Michael R. Ziebell [a,b,1], Zhan-Gong Zhao [b], Bai Luo [c], Yi Luo [b], Eva A. Turley [d], Glenn D. Prestwich [b,e,*]

[a] *Department of Physiology and Biophysics, The University at Stony Brook, Stony Brook, NY 11794-8661, USA*
[b] *Department of Medicinal Chemistry, The University of Utah, 30 South 2000 East, Room 201, Salt Lake City, UT 84112-5820, USA*
[c] *Huntsman Cancer Institute, 2000 Circle of Hope, Room LL376, The University of Utah, Salt Lake City, UT 84112-5550, USA*
[d] *London Regional Cancer Centre, Cancer Research Laboratories, Department of Oncology, 790 Commissioners Road East, London, ON, Canada N6A 4L6*
[e] *Center for Cell Signaling, 421 Wakara Way, Suite 360, Salt Lake City, UT 84108, USA*

Received 3 May 2001; revisions requested 26 June 2001; revisions received 14 August 2001; accepted 30 August 2001
First published online 1 October 2001

Abstract

Background: Hyaluronan (HA) is a non-sulfated glycosaminoglycan (GAG) that promotes motility, adhesion, and proliferation in mammalian cells, as mediated by cell-surface HA receptors. We sought to identify non-carbohydrate ligands that would bind to and activate cell-surface HA receptors. Such analogs could have important therapeutic uses in the treatment of cancer, wound healing, and arthritis, since such ligands would be resistant to degradation by hyaluronidase (HAse).

Results: Peptide ligands that bind specifically to the recombinant HA binding domain (BD) of the receptor for hyaluronan-mediated motility (RHAMM) were obtained by screening two peptide libraries: (i) random 8-mers and (ii) biased 8-mers with alternating acidic side chains, i.e. XZXZXZXZ (X = all-L-amino acids except Cys, Lys, or Arg; Z = D-Asp, L-Asp, D-Glu, or L-Glu). Selectivity of the peptide ligands for the HABD was established by (i) detection of binding of biotin- or fluorescein-labeled peptides to immobilized proteins and (ii) fluorescence polarization of FITC-labeled peptides with the HABD in solution. HA competitively displaced binding of peptides to the HABD, while other GAGs were less effective competitors. The stereochemistry of four biased octapeptides was established by synthesis of the 16 stereoisomers of each peptide. Binding assays demonstrated a strong preference for alternating D and L configurations for the acidic residues, consistent with the calculated orientation of glucuronic acid moieties of HA.

Conclusions: Two classes of HAse-resistant peptide mimetics of HA were identified with high affinity, HA-competable binding to the RHAMM HABD. This demonstrated that non-HA ligands specific to a given HA binding protein could be engineered, permitting receptor-specific targeting.

Keywords: Glycosaminoglycan-mimicking peptide; High-affinity ligand; Hyaluronan binding domain; Receptor for hyaluronan-mediated motility

1. Introduction

The extracellular matrix polysaccharide hyaluronan (β-1,4-GlcUA-β-1,3-GlcNAc-)$_n$ (hyaluronic acid, or simply HA) is a non-sulfated glycosaminoglycan (GAG) that promotes cell motility, adhesion, and proliferation in mammalian cells [1], thereby playing roles in morphogenesis [2], wound healing [3] and metastasis [4]. These functions are mediated by cell-surface HA receptors, which initiate key cell signaling cascades when activated by HA, leading to physiological changes [4]. Non-carbohydrate ligands that would bind to and activate cell-surface HA receptors could have important therapeutic uses in the treatment of cancer, wound healing, and arthritis, since such ligands

Abbreviations: bHA, biotinylated hyaluronic acid; BD, binding domain; CS, chondroitin sulfate; erk1, extracellular signal-regulated protein kinase; FAK, focal adhesion kinase; Fmoc, 9-fluorenylmethoxycarbonyl; FP, fluorescence polarization; GAG, glycosaminoglycan; GST, glutathione *S*-transferase; HA, hyaluronic acid or hyaluronan; HABD, hyaluronic acid binding domain; HAse, hyaluronidase; PBS, phosphate-buffered saline; mP, millipolarization units; PVP-40, polyvinyl pyrrolidone; RHAMM, receptor for hyaluronan-mediated motility; SA–HRP, streptavidin–horseradish peroxidase; TBS, Tris-buffered saline; TMB, 3,3′,5′,5-tetramethylbenzidine

[1] Present address: Department of Neurobiology, Harvard Medical School, 220 Longwood Avenue, Boston, MA 02115, USA.

* Corresponding author.
E-mail address: gprestwich@deans.pharm.utah.edu (G.D. Prestwich).

1074-5521/01/$ – see front matter
PII: S1074-5521(01)00078-3

would be resistant to degradation by hyaluronidase (HAse). To this end, two peptide libraries were prepared and screened to identify high-affinity ligands for the HA receptor RHAMM (receptor for hyaluronan-mediated motility).

RHAMM mediates cell migration and proliferation in many normal cells and in tumor cell-lines [5]. Isoforms of RHAMM are functionally active both in the cytoplasm and on the cell surface [4]. The extracellular forms of RHAMM appear to act as co-receptors, which modulate signaling through integral receptors, such as the PDGF receptor [6–8]. RHAMM requires the small GTPase p21 ras and pp60 src to promote motility [8,9]. A target of src-regulated phosphorylation is focal adhesion kinase (FAK) ($pp125^{FAK}$), which is an important integrin binding protein. Phosphorylation of FAK leads to focal adhesion turnover, a critical step in cell locomotion [10].

RHAMM occurs naturally as a functional HA receptor in primary human endothelial cells [11] and is overexpressed as several isoforms in human tumors and tumor cell-lines including colorectal [12], breast [13,14], pancreatic [15], and multiple myeloma [16]. A dominant negative mutant of RHAMM, possessing a non-functional HA binding domain (BD), can block cell transformation by mutant active ras. Furthermore, overexpression of one RHAMM isoform constitutively activates the kinase erk1 (extracellular signal-regulated protein kinase) [7] and is transforming in fibroblasts [10]. RHAMM occurs as an intracellular protein but can be expressed on the cell surface, a condition observed most often in single cells such as leukocytes [17,18] and in subconfluent fibroblasts [7]. Cell-surface RHAMM binds to extracellular HA and the HA–RHAMM complex undergoes receptor-mediated endocytosis [19]. Intracellular RHAMM binds to cytoskeletal proteins [20] and associates with proteins in the erk kinase cascade [7].

Mutational analysis of RHAMM identified two regions near the C-terminus that are required for full HA binding [21]. These regions have clusters of basic residues and have a so-called BX_7B motif (B = basic residue, X = any non-acidic residue) present in several HA binding proteins [22]. Synthetic peptides representing the RHAMM domains inhibit HA binding to full length RHAMM, while peptides representing other parts of the primary sequence fail to inhibit binding [21]. RHAMM has one of the highest densities of basic residues of any HA receptor. CD44 and other link module-containing proteins may have the BX_7B motif, but these HABDs are architecturally and functionally distinct [23]. Although RHAMM is known to bind heparin at the same binding site as HA [24], no other GAGs have been reported to bind to RHAMM with high affinity.

The secondary structure of RHAMM is predicted to be predominantly helical. The structure of the HABD was recently studied using multi-dimensional nuclear magnetic resonance (NMR) and was observed at 3 Å resolution to be a helix-loop-helix with a coiled-coil tertiary structure [25]. This contrasts with the β-sheet-containing link module of the protein TSG-6 [26,27]. Using RHAMM numbering [28], the N-terminal of the HABD is completely contained within a loop (residues 531–539), while the second half of the domain (residues 553–562) spans a loop and a helical region. The interaction of HA with HABDs requires both electrostatic interactions between the glucuronate carboxylates and basic residues of the protein, as well as potential hydrophobic interactions involving methine patches on HA [27].

In this study, two synthetic peptide libraries, one composed of random octapeptides and one containing alternating acidic and non-acidic residues, were examined for potential non-GAG ligands for the HABD. These one-bead, one-peptide libraries [29] were screened with the RHAMM–HABD in order to identify high-affinity peptides for the HABD. The biased acidic library was designed to mimic the natural pattern of alternating glucuronic acid carboxylates present in HA; this represents the first rational approach to identification of a non-GAG ligand for a HA binding site. Importantly, this library included both natural and unnatural configurations of the acidic residues to further explore possible oligosaccharide conformations that could be important in ligand recognition.

This paper will present three major results. First, recurring peptide motifs that bind to HABDs were identified in both biased and random libraries. Second, solid-phase binding and fluorescence polarization (FP) assays were developed to quantify the relative affinity and selectivity of peptide–RHAMM interactions. Third, the importance of including acidic amino acids with unnatural configurations was demonstrated. A molecular model based on minimized structures of the active enantiomeric peptides suggested that the staggered carboxylate orientation relative to the peptide backbone is similar to the carboxylate orientation in HA.

2. Results

2.1. Initial library screening

A solid-phase method was employed to confirm that RHAMM HABD-containing proteins would bind to biotinylated HA (bHA), based on earlier methods used for bHA–HABD studies [30,31]. To this end, a dot blot of purified glutathione *S*-transferase (GST)–RHAMM(518–580), GST, and RHAMM(518–580) on polyvinyl difluoride (PVDF) membrane was employed, since the highly basic, small RHAMM(518–580) polypeptide itself failed to electrotransfer to PVDF. GST–RHAMM(518–580) and RHAMM(518–580) bound bHA, but neither GST alone nor bovine serum albumin (BSA) bound bHA (data not shown). Comparison of electrotransferred pro-

teins on PVDF with electrophoretically separated GST–RHAMM(518–580) and thrombin-cleaved GST–RHAMM(518–580) (only GST remained) showed that the fusion protein could be detected with bHA (data not shown) while GST alone could not. Similarly, thrombin cleavage of GST–RHAMM(518–580) in a 96-well plate released the HABD, which was detected using a dot blot. These control experiments demonstrated the specificity of HA binding to RHAMM(518–580) and not to the GST domain.

Two eight-amino acid libraries were synthesized on 100-μm Tentagel beads and screened using GST–RHAMM(518–580) as the HABD. Library **R** contained completely random sequences of 19 L-amino acids (excluding Cys), while Library **B** consisted of alternating acidic residues in an XZXZXZXZ pattern. For Library **B**, the acidic (Z) residues were allowed to have either the natural L or unnatural D absolute configuration. The synthesis generated three million beads for each library; typically, an aliquot of ca. 100 000 beads was used for each screen. The number of beads was determined by the practical limits of the experimental approach, and by the calculation that this number should adequately represent the dipeptide or tripeptide motifs that were anticipated in an octapeptide population. Thus, starting with 100 000 beads, approximately 30 positive 'blue' beads were identified after three rounds of screening. The final round of screening included a competition step with HA to block peptide binding to the HABD; positive beads in this step were 'white'. Table 1 also summarizes the peptides directly sequenced following screening of Libraries **R** and **B** with GST–RHAMM(518–580). Approximately half of the positive beads were sequenced, and of these, 20% of the sequencing attempts failed for technical reasons. A single 'white' bead from the first screening was selected as a negative control; peptide **NB** had the sequence IDSDWEGE.

Table 1
Sequences of HA-mimetic peptides

Random		Biased	
R-1	SGRPYKPP	**B-1**	MDYEPEQE
R-2	YXSSNKPG	**B-2**	YDSEYESE
R-3	EGEWPVYP	**B-3**	FDFDSEYE
R-4	WNYTEAKG	**B-4**	EDAENDEE
R-5	QAMNKFTF		
R-6	NTDSNKNM	**NB**	IDSDWEGE
R-7	NPVFNDGY		
R-9	FLRWFIMI		
R-10	EMAQMLLE		
R-11	PFLMKFPI		
R-12	IYIYPQPQ		

Peptide sequences were obtained by direct Edman degradation using positive library beads screened with RHAMM(518–580). Peptide **NB** sequence was obtained from a negative control (non-binding) bead selected from the first round of screening of Library **B**.

*2.2. Deconvolution of Library **B** hits*

Since Library **B** was synthesized with either the D- or L-isomers at the alternating acidic residues, it was necessary to deconvolve the particular combination of natural and unnatural amino acids in each positive hit. Solid-phase synthesis on each bead created one of 16 possible diastereoisomers of a given 'letter' sequence, corresponding to a total of two enantiomers at each of four positions. Using automated Edman degradation for peptide sequencing, the chirality of the PTH amino acid sequenced at any given cycle could be determined. Prior to μmol-scale synthesis of peptides to determine binding affinities, the diastereomeric ambiguity was first resolved by construction of a mini-library of the 16 individual diastereomers of the Library **B** peptides. This peptide mini-library was constructed as an array of spots on a cellulose membrane (Pepspots®), in which each spot contained a single diastereomer of the Library **B** peptide letter sequence (3–5 nmol/spot). The membrane mini-library was prepared commercially, and consisted of an array of 72 spots: 16 diastereomers of peptides **B-1**, **B-2**, **B-3**, and **B-4**, four negative control spots (using the sequence of a non-binding negative control, IDSDWEGE), and four spaces between each set of 16 diastereomers.

GST–RHAMM(518–580) binding to the Pepspots® mini-library was carried out by semi-dry transfer in order to permit use of the original membrane for multiple protein-stripping and reprobing experiments. Thus, GST–RHAMM(518–580) was incubated with the blocked Pepspots® membrane and specifically bound protein was transferred to a PVDF membrane. Bound GST–RHAMM(518–580) was detected using goat anti-GST, followed by anti-goat IgG horseradish peroxidase (HRP)-conjugated antibodies. Binding was visualized and quantified (Fig. 1) with a chemiluminescent HRP substrate. These data allowed selection of specific diastereomers of Library **B** peptides to analyze binding of a single homogeneous species rather than a diastereomeric mixture. Four pairs of diastereomers with ca. 100-fold binding differences were synthesized and used as described below to measure binding affinities for the RHAMM HABD (see Table 2).

The data in Fig. 1 illustrate that peptide diastereomers containing only L-Glu and L-Asp do not exhibit the optimal affinity. This most likely reflects the importance of the orientation of the carboxylate-containing side chains. With a combination of D- and L-amino acids in a single peptide, the structures with carboxylates on alternating 'sides' of the peptide more closely imitate the orientation of the glucuronate carboxylates in HA. The **B-1**, **B-3** and **B-4** series demonstrate this clearly, in that the all-L-peptide exhibits no observable binding. The all-L-peptide in **B-2** bound with lower affinity than diastereomers containing a single D-Asp or D-Glu residue. This suggests that one component of binding is derived from the hydrophobic

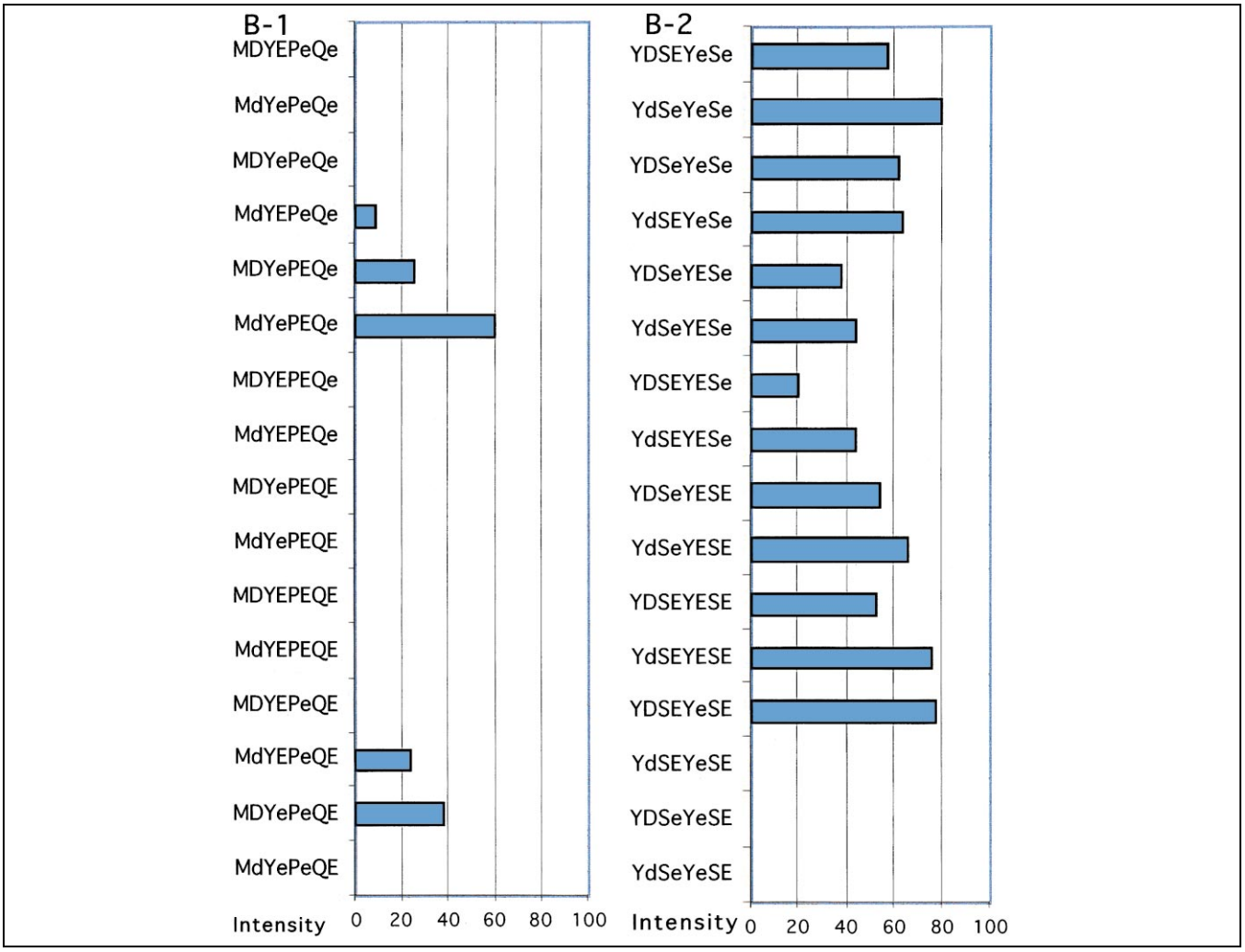

Fig. 1. Deconvolution of Library **B** diastereoisomers. Uppercase letters represent the natural L-configurations and lowercase letters represent the D-configurations of Glu (E, e) and Asp (D, d). Peptides were synthesized as 5 nmol 'Pepspots®' and transferred to PVDF as described in the text. A chemiluminescence assay with a HRP-labeled secondary antibody was used to detect GST–RHAMM(518–580) bound to each peptide spot. The intensity of each spot was quantified with NIH Image software. Data shown are from a single film, but the results were validated from three blots.

repeats as well as charge orientation. Similarly, the aromatic residue-rich **B-3** peptides showed robust binding to the HABD, as favored by the 'opposite side' carboxylate orientation. Hydrophobic and aromatic-rich patches on HA have been implicated in stabilizing HA secondary structure [32,33] and in HA–HABD interactions [23,34].

2.3. Affinities of peptides for RHAMM HABD

Three microplate binding assays were employed to measure the affinity of synthetic peptides for RHAMM(518–580): enzyme-linked immunosorbent assay (ELISA), a fluorescence-based analog of the ELISA, and FP. The ELISA required a biotinylated peptide, while both the fluorescence-based solid-phase and the FP assays required a fluorophore-modified peptide. Thus, two thiol-reactive maleimide reporter groups were used, requiring an N-terminal cysteine for probe attachment. For competition assays with probe-modified peptides or bHA, peptides lacking the Cys residue were also required. These were conveniently prepared by removal of half of the synthetic peptide from the synthesizer prior to addition of the final Cys residue. Synthetic peptides from each sub-group of similar peptides of Library **R** were prepared (see Table 1). For Library **B**, each of the four positive peptides containing both D- and L-acidic residues, as identified by the Pepspots® deconvolution experiment, were synthesized.

The binding affinities of the synthetic peptides were measured with the ELISA method as described in Section 5, and K_D values were determined mathematically [35]. In a typical experiment, the K_D for a given biotinylated peptide was determined using successive five-fold dilutions of probe and using a fixed amount of immobilized protein. Experiments were performed in triplicate with background (no protein) subtraction prior to calculations. The stoichiometry of binding was determined using a standard curve of streptavidin (SA)–HRP serial dilutions. For example, **R-3**, one of the highest affinity random peptides, had a

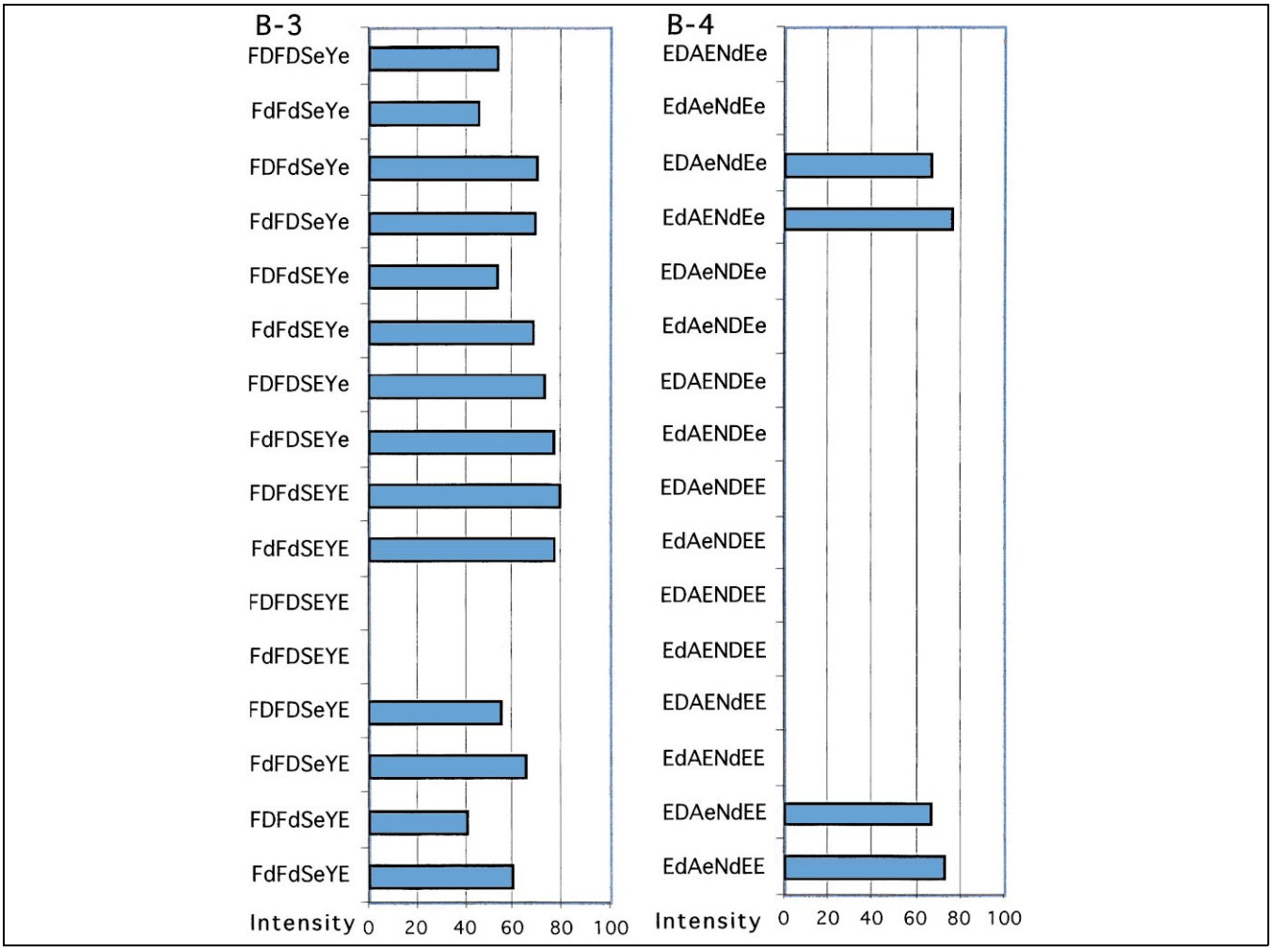

Fig. 1 (*Continued*).

Table 2
Binding affinities for synthetic HA-mimetic peptides

Name	Sequence	Binding displaced by HA (%)	K_D from plate assay (nM)	K_D from FP (nM)
Library **B**				
B-1A	CMdYEPeQe	33 ± 5	49 ± 3	17 ± 5
B-1B	CMDYePEQe	61 ± 8	73 ± 5	nd
B-2A	CYDSeYeSe	76 ± 5	8 ± 1	nd
B-2B	CYDSEYeSE	78 ± 8	74 ± 8	nd
B-3A	CFDFdSEYe	86 ± 7	730 ± 25	nd
B-3B	CFdFdSEYE	67 ± 10	1400 ± 200	nd
B-4A	CEDAeNdEe	37 ± 8	110 ± 13	nd
B-4B	CEdAENdEe	53 ± 5	499 ± 75	220 ± 58
Library **R**				
R-3	CEGEWPVYP	67 ± 5	48 ± 2	nd
R-5	CQAMNKFTF	58 ± 5	270 ± 45	nd
R-12	CIYIYPQPQ	75 ± 9	5300 ± 85	nd

An N-terminal Cys was added to each bead-derived sequence to permit attachment of reporter groups. The K_D values from the plate assay were obtained using the solid-phase ELISA using N-terminally biotinylated peptides as described in the text. Competitive displacement was determined by pre-incubation of RHAMM–HABD with 1 mg/ml of 4–40 kDa HA. In the amino acid sequences, uppercase letters represent the natural L-configurations and lowercase letters represent the D-configurations of Glu (E, e) and Asp (D, d). Key: nd = not determined.

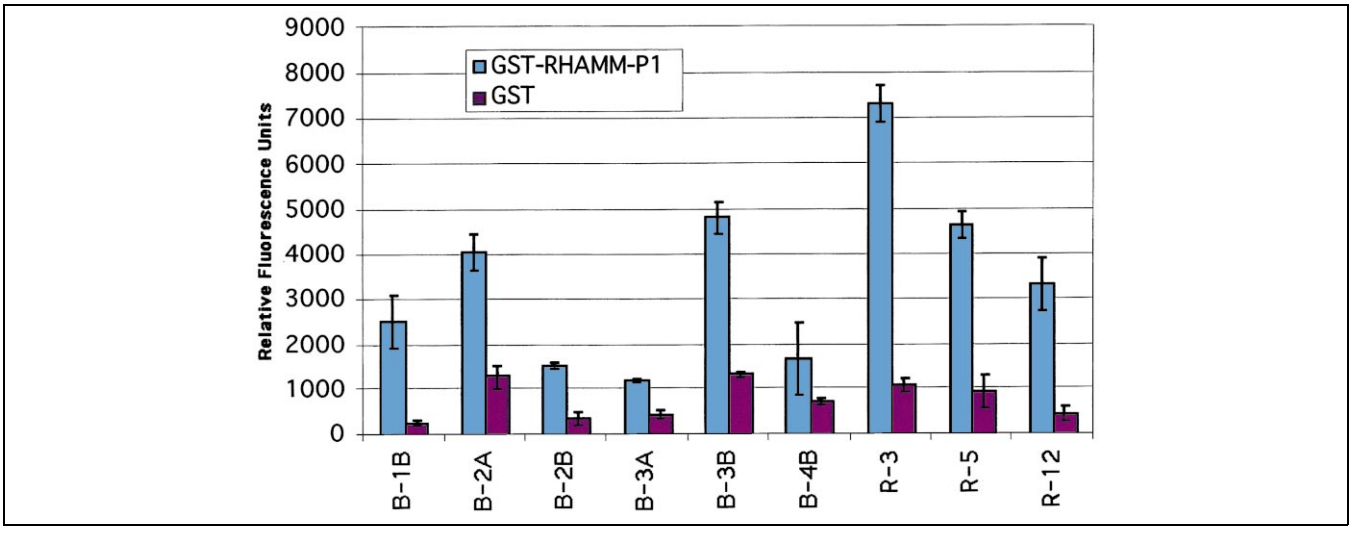

Fig. 2. Binding of nine fluorescein-labeled peptides to GST–RHAMM(518–580) and GST alone using the solid-phase fluorescence binding assay.

K_D value of 48 nM with a 1:1 binding ratio; biased peptide **B-2A** had a K_D value of 8 nM. The binding affinities are summarized in Table 2.

2.4. *Domain selectivity and competitive displacement of peptide binding by GAGs*

The ELISA was modified to address selectivity of binding. Thus, a domain selectivity and a GAG competition assay were each conducted using a modification of the solid-phase ELISA that allowed use of fluorescein-labeled peptides. Although the data from this modification are less accurate for absolute quantitation, a lower background could be achieved as compared to the SA–HRP ELISA method. First, we demonstrated that RHAMM HABD, not the GST fusion partner, was responsible for peptide binding. Peptides from the two libraries were evaluated. Fig. 2 illustrates that the majority of peptides show negligible binding to the GST domain. It is possible that the fluorophore modification could increase the non-specific binding beyond that detected in the original library screening protocols.

Second, we evaluated the effectiveness of several GAGs to inhibit binding of synthetic peptides to the HABD of RHAMM. HA was used as a competitor for all synthetic peptides, and other GAGs were evaluated with a subset of peptides. Fluorescein-labeled peptides representing each of the libraries were added to ELISA plates containing immobilized GST–RHAMM(518–580) that had been pre-incubated with 4–40 kDa HA, and washed to remove excess ligand. Fig. 3a shows the competitive displacement of peptide binding to GST–RHAMM(518–580) by HA for six selected peptides. In all but one instance, 0.1 mg/ml of the 4–40 kDa HA provided optimal competition of the

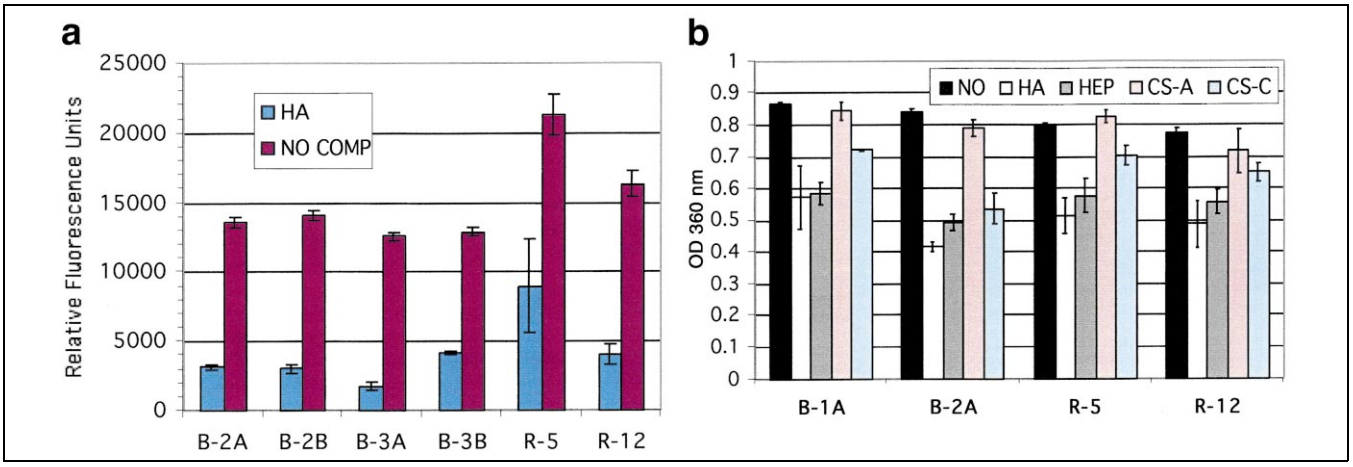

Fig. 3. a: Competitive displacement of six selected fluorescein-labeled peptides (**B-2A**, **B-2B**, **B-3A**, **B-3B**, **R-5**, and **R-12**) by HA using the solid-phase fluorescence binding assay. The concentration of 4–40 kDa HA was 0.1 mg/ml, except for **B-2A**, for which 1 mg/ml of 4–40 kDa HA was used. b: Competitive displacement of biotinylated peptide binding to GST–RHAMM(518–580) by HA and three sulfated GAGs using the solid-phase colorimetric ELISA for four selected biotinylated peptides (**B-1A**, **B-2A**, **R-5**, and **R-12**). Key: HEP, heparin; CS-A, chondroitin 4-sulfate; CS-C, chondroitin 6-sulfate.

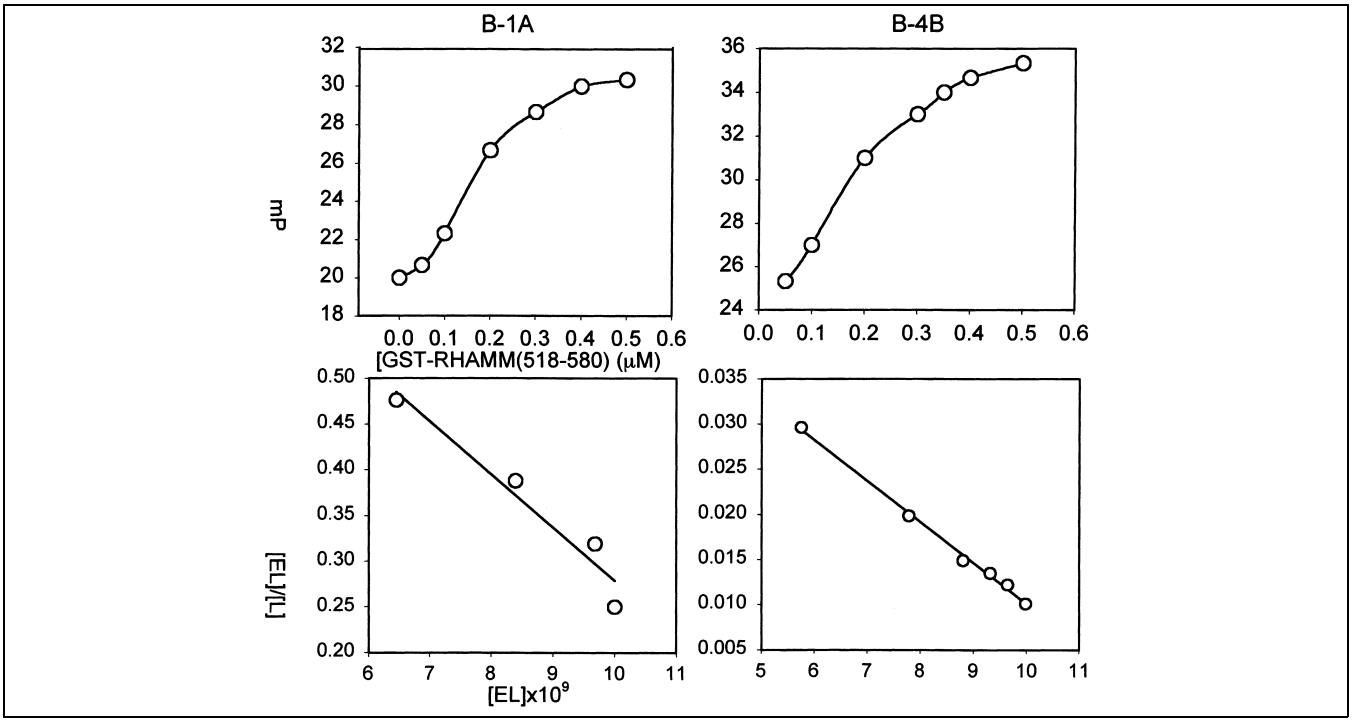

Fig. 4. Binding curves and Scatchard analyses of FP measurements of GST–RHAMM(518–580) with peptides **B-1A** and **B-4B**.

peptide. For the highest-affinity peptide **B-2A**, 1 mg/ml of 4–40 kDa HA was necessary to compete for peptide binding. Fig. 3b illustrates the relative competitive displacement by HA and three sulfated GAGs for four selected peptides; in this ELISA assay, the biotinylated peptides were employed in conjunction with the SA–HRP reporter system. The data in Fig. 3b show an overall higher background than those in Fig. 3a as a result of additional non-specific interactions from the secondary ELISA detection system. The non-specific interactions of both HA and chondroitin sulfate (CS) with BSA are well known [36,37]. The colorimetric detection system was used for experiments in Fig. 3b rather than fluorescence to be consistent with the binding assay used for the majority of the peptide binding. The differences in competition between CS-A and CS-C are noteworthy, since these 4-sulfate (CS-A) and 6-sulfate (CS-C) regioisomers of CS interact differently with different HA binding proteins [14,38–40]. Preliminary data from our laboratories indicated that CS-A showed modest, but higher affinity to RHAMM than CS-C.

2.5. FP assays to verify solid-phase binding results

The data from the solid-phase binding assays were supplemented by a second methodology. FP measures the change in anisotropy of a fluorescent probe in free and bound states [41–43]. An increase in anisotropy is proportional to the ligand–protein complex formation; this assay is independent of fluorescence intensity. Using a fixed concentration of each fluorescein-labeled peptide, increasing concentrations of the RHAMM–HABD were added to a 96-well plate optimized for low-background fluorescence measurements. The concentrations were chosen so that the measurements span the range from $0.01 \times K_D$ to $100 \times K_D$. Fig. 4 illustrates the primary data for peptides **B-1A** (17 ± 5 nM), and **B-4B** (220 ± 58 nM), which showed affinities of 49 nM and 499 nM, respectively, in the ELISA assay. This correlation validated the FP assay for use in measuring peptide–protein interactions for HA-mimicking peptides. However, due to the multivalent nature and viscosity-altering properties of HA, it was not practical to use the FP assay for competitive displacement experiments.

3. Discussion

The importance of RHAMM in cell motility and metastatic progression [12,13] provided the impetus to identify potential non-GAG ligands that could serve as HAse-resistant HA surrogates in basic research and as leads for drug design. We sought ligands that could specifically target the HABD of RHAMM but would not be recognized by other hyaladerins such as CD44 and link protein. We reasoned that peptide mimics can explore conformations and chemical functionalities unavailable to natural GAG ligands. Consequently, peptide mimics could achieve novel selectivities for binding to, and activation of, different HA receptors. To this end, two peptide libraries were screened using the HABD of RHAMM as bait for octapeptides with high affinity and selectivity. Both libraries afforded high-affinity ligands that acted as HA surrogates, as deter-

mined by three in vitro binding assays. Library **B**, which contained alternating acidic residues, was inspired by the alternating pattern of glucuronic acid and *N*-acetylglucosamine that characterizes the linear HA structure. Moreover, we anticipated that nucleophile-rich residues would be commonly found in the HA-mimetic peptides identified by this screen. In contrast, we identified common motifs in which hydrophobic residues predominated in Library **R**, a bead-based library of random octamers. This unexpected result was nonetheless consistent with the observation that HA can interact with aromatic-rich patches on another HA binding protein, the link module of human TSG-6 [34]. Thus, the two different peptide libraries provided both rational and unbiased approaches to ligand identification.

3.1. The random bead library has tripeptide motifs

Three recurring dipeptide or tripeptide motifs were noted in Library **R**: (i) the PV¥ motif, where ¥ is F or Y, was present in **R-7** and **R-3**; (ii) the QAM motif was present in **R-5** and in retrograde form in **R-10**; and (iii) the P¥/¥P dipeptide sequence was found in **R-1**, **R-11**, and **R-12** (Table 3). Of these random library-derived ligands, the peptide with the highest affinity for RHAMM-(518–580) was **R-3** (EGEWPVYP) with an apparent K_D value of 48 nM. Interestingly, the negative control peptide **NB** (IDSDWEGE) shared the EGE tripeptide, which thus appeared not to participate in binding; this provided additional support for the importance of the PV¥ motif in binding to RHAMM. Moreover, **R-3** contained a P¥/¥P motif, which could further enhance the affinity of this peptide.

Since the structure of the RHAMM(518–580) showed the HABD to be a surface-exposed domain [25], peptide binding could be governed by a short motif; this would account for the sequence diversity within the peptide ligands identified. In addition, differences in solubility and elements of secondary structure could affect relative binding affinities. It is surprising that few peptides were represented in both libraries. Only one Library **R** peptide showed the acidic-X-acidic motif imposed synthetically on the Library **B**, and in that example, the EGE may not even be important for binding. The results from the Library **B** peptides and the importance of alternating absolute configurations of the acidic side chains can account for this apparent paradox, as described below.

Table 3
Alignment of random peptide sequences showing tri- and dipeptide motifs

NPVFNDGY EGEWPVYP	R-7 R-3
ELLMQAME QAMNKFTF	**R-10** retrograde R-5
PPKYPRGS EGEWPVYP PFLMKFPI IYIYPQPQ	**R-1** retrograde R-3 R-11 R-12

The P¥/¥P motif also occurred in peptides screened with the link module-containing HA binding protein TSG-6 [26]. TSG-6 is a 275-amino acid secretory protein involved in cell–cell and cell–matrix interactions during inflammation [44], and a three-dimensional solution structure of the HA binding link module has been determined by NMR [26]. None of the peptides obtained with this structurally different 'bait' protein bound to GST–RHAMM(518–580), and these data will be presented in due course (M.R. Ziebell, A.J. Day, and G.D. Prestwich, unpublished results).

3.2. Precedent for alternating charged D- and L-amino acids in the biased library

The rationale for synthesizing Library **B** with alternating acidic amino acids was to mimic the alternation of glucuronic acids of HA, in both the linear and three-dimensional distribution of charge. The glucuronic acid moieties of HA are separated by approximately 10 Å [45], with a dihedral angle between −110° and −167°, indicating that they protrude from opposite faces of a plane that approximates the linear sequence of sugars. Since these charge repeats appear to be important in HA–protein interactions, Library **B** was designed to detect peptides with alternating carboxylates with high affinity for RHAMM–HABD. To this end, Library **B** was prepared with either D- or L-enantiomers of Glu or Asp in the acidic residue position.

A non-optimized model of a random coil peptide suggested that alternating acidic residues should give a pattern of negative charges separated by approximately 10 Å. A model was thus constructed based on diastereomers discovered from the library screen. The peptides **B-2** (YDSEYESE) and **B-2B** (YDSEYeSE) were modeled using InsightII (Molecular Simulations, Inc.). From a family of 10 conformers, each minimized and subjected to a routine molecular dynamics protocol, a marked difference in the orientation of the acidic side chains was apparent (Fig. 5). The average distance between Glu4 HE2 and Glu6 OE1 for **B-2** was 6.11 ± 1.72 Å, while for **B-2B** this distance was 12.56 ± 1.47 Å. The averages of the absolute value of the dihedral angles between Glu4 and Glu6 side chains were $41.9 \pm 29.6°$ for **B-2** and $129.5 \pm 44.2°$ for **B-2B**. These parameters suggest that a peptide with alternating acidic residues, one with D configuration and one with L configuration, should most closely mimic HA. The results of this series of minimizations are graphically represented in Fig. 5, where each point represents the mini-

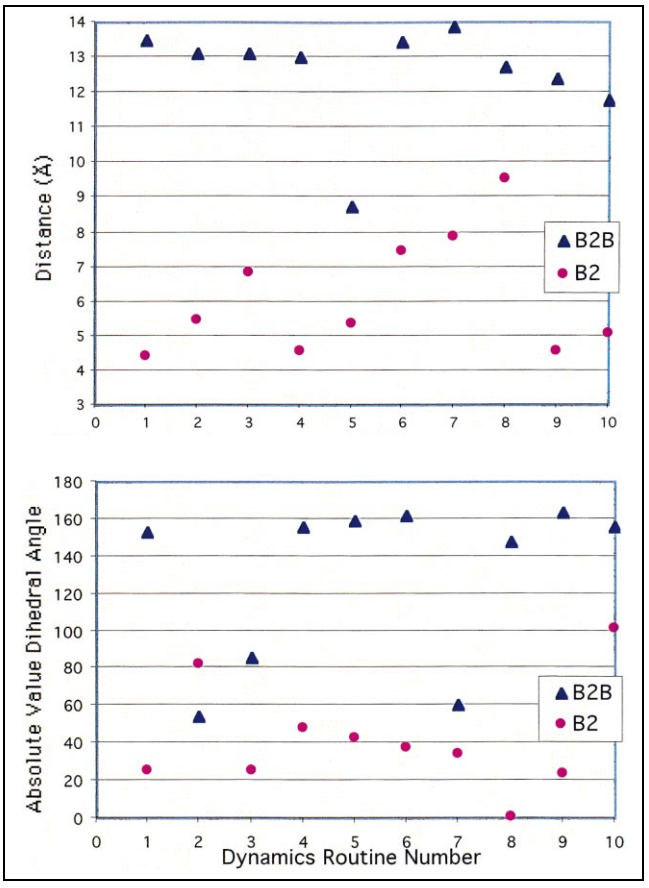

Fig. 5. Summary of 10 molecular dynamics and minimization routines on peptides **B-2** and **B-2B**. The distance is measured between Glu4 HE2 and Glu6 OE1 on either peptide. The modeling was performed using Discover and included 1000 iterations of minimization runs using an Amber force field. The dynamics routine had 10 000 steps including charge and Morse terms.

mized distance between the two protons. Fig. 6 illustrates three structures obtained from the molecular modeling experiments. Coordinates for HA (Fig. 6, top) were obtained from the Protein Databank (accession no. 4HYA) [45] with the glucuronic acid sugar residues highlighted. The calculated structures for the all-L-configuration octapeptide **B-2** (center) and the peptide with a single D-configuration side chain **B-2B** (bottom) showed the distance and angular relationships between acidic side chains. In the minimum energy conformer for **B-2**, these constants poorly imitated HA; in contrast, the minimum energy conformer for **B-2B** more adequately approximated the spatial and angular measurements of a HA oligosaccharide.

3.3. The biased library favors unnatural acidic residues

A number of high-affinity 'hits' were sequenced from beads in Library **B**. However, even though each hit was a unique molecular species, the Edman degradation could not provide information on the absolute configuration of the particular linear sequence obtained. Thus, each sequence represented 16 possible molecular structures. Deconvolution was accomplished by synthesis of each of the 16 diastereomers of three Library **B** peptides using the commercial Pepspots® technology. The strongest binding peptides from the biased library were specific diastereomers of peptides **B-1** (MdYEPeQe, peptide **B-1A**) and **B-2** (YDSeYeSe, peptide **B-2A**); D-amino acids are indicated with lower case letters. Peptides with alternating D- and L-acidic residues showed the highest affinity. The 'anti' relationship appeared to most closely reflect the angular orientation of carboxylates on HA, consistent with the model used to design these HA-mimetic peptides. In Library **B**, we deliberately created a pattern of charges within each octapeptide. While many octapeptides bound with high affinity to the RHAMM HABD, charge distribution was not the only factor dictating binding affinity, as previously observed for Library **R** peptides.

Small aromatic residues (Tyr or Phe) and Ser residues were abundant in Library **B**, e.g. **B-2** (YDSEYESE) and **B-3** (FDFDSEYE). The aromatic residues may mimic the putative hydrophobic patches of HA. In peptides with alternating D- and L-acidic side chains as well as Tyr, Phe, or Ser (e.g. peptide **B-3A**, FDFdSEYe), the random

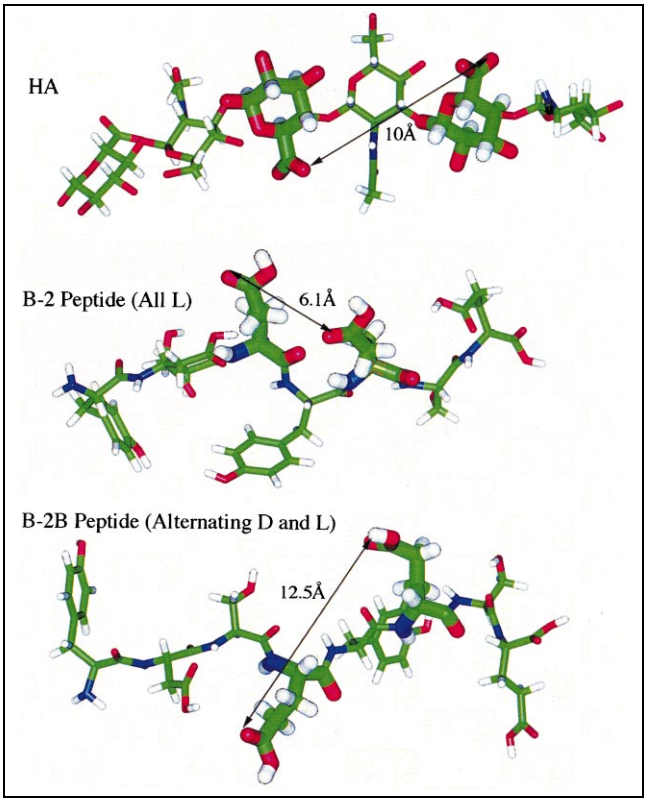

Fig. 6. Molecular model showing calculated minimum energy structures for HA (top), peptide **B-2**, YDSEYESE (middle, all-L-amino acids), and peptide **B-2B**, YDSEYeSE (bottom), which contains a single D-Glu residue. The carboxylate to carboxylate distances are indicated by double-headed arrows in each energy-minimized structure.

coil conformation predicts that the polar and non-polar side chains would be oriented at a 180° dihedral angle. The formation of a hydrophobic surface consisting of two phenyl rings could reflect the conformation of HA in which the eight methines on the hydrophobic face span three sugar residues. Modeling of these peptides into a three-dimensional model of RHAMM is in progress [25].

In summary, a fusion protein was generated that contains a 62-amino acid polypeptide comprising the HABD of RHAMM [46]. This RHAMM construct was shown to have HA binding activity and the purified protein had defined secondary and tertiary structures [25]. Using this HABD as 'bait', two peptide libraries were screened for molecules that specifically target the HABD of RHAMM. Several of the peptide hits that were identified and sequenced were then synthesized and evaluated to determine their affinity and specificity in binding to RHAMM. Many of these peptides bound to RHAMM with high affinity, and competition by HA or other GAGs suggested that the peptides were directed to the HABD.

4. Significance

We have identified two classes of HAse-resistant peptide mimetics of HA that exhibit high-affinity, HA-competable binding to RHAMM, a receptor important in cell motility, adhesion, and proliferation and implicated in the pathology of cancer. These peptides may serve as antagonists that could block the transforming potential of RHAMM. In related work, we also identified a number of 15-mer peptides by phage display that bind with high affinity to RHAMM(518–580) and affect cell physiology and erk1–RHAMM interactions [47]. In an analogous experiment, phage-derived peptides that bound the CTLA4 receptor were found to activate T-cells [48].

Peptides that mimic HA could also be useful for drug targeting. The problem of directing anti-cancer agents to tumors remains one of the technological barriers to developing effective therapies for cancer treatment [49]. The overexpression of RHAMM on cancer cells relative to normal epithelial cells provides an opportunity for tumor-specific drug targeting. HA-conjugated anti-tumor agents [50] and other drugs [51] often lack specificity for a particular class of HA receptors.

Either as therapeutics or targeting moieties, HA-mimetic peptides offer several unique properties. First, the peptides are resistant to HAse degradation. Second, peptides can act as antagonists rather than agonists. Third, peptides can be selected that would not be recognized by liver endothelial cell receptors involved in HA clearance from circulation [52]. Fourth, peptides could be selected to be specific for RHAMM isoforms or CD44 isoforms present in pathological situations.

5. Materials and methods

5.1. Sub-cloning of RHAMM(518–580) into PGEX-2T

The RHAMMv4 cDNA in a pCRII vector [10] was used as a template for PCR production of the RHAMM constructs. Sequence-specific primers encoded restriction sites to permit ligation of PCR products into the appropriate vectors. Thus, the RHAMM(518–580) PCR product was digested, purified, and ligated directly into PGEX-2T (Pharmacia) using unique *Eco*RI and *Bam*HI restriction sites. Initial ligation of PCR products into a PGEM-T vector (Novagen) improved the ligation efficiency. Plasmid and PCR insert purification followed standard protocols, and DNA was purified by either phenol–chloroform extraction [53] or with Qiagen columns.

5.2. Purification of GST fusion protein

GST–RHAMM(518–580) (RDSYAQLLGHQNLKQKIKHVVKLKDENSQLKSEVSKLRSQLVKRKQNELRLQGELDKALGIR) [28,46], with BX_7B motifs underlined, was expressed in BL21 *Escherichia coli* cells in ampicillin-containing media by induction with IPTG (2 mM). Cells were harvested by centrifugation at $2000 \times g$ for 30 min, resuspended in phosphate-buffered saline (PBS) with 30 μg/ml leupeptin and 1 mM PMSF, and lysed using a French press at 20 000 psi. Triton X-100 (1% final concentration) was added to the lysate, incubated on ice for 30 min, and centrifuged at $12\,000 \times g$ for 30 min. The brown supernatant was applied to 10 ml of glutathione Sepharose equilibrated in PBS at 4°C, the column was washed with 15–20 ml of PBS at 1 ml/min, and the GST–RHAMM(518–580) was eluted with 50 mM glutathione, 10 mM Tris, pH 8.0. Glycerol was added to 10% final concentration, and 1.5-ml aliquots of purified protein were flash frozen on dry ice and stored at −30°C. Then, a sample was thawed in ice water and diluted to the required concentration in Tris-buffered saline (TBS). Unused protein from a thawed aliquot was discarded; no loss of activity was noted for a single freeze-thaw cycle.

5.3. Synthesis of bHA

bHA was prepared using the hydrazide method [54,55]. Bacterially expressed HA (100 mg, 0.25 mmol disaccharide equivalents, molecular weight 700 000) (Clear Solutions Biotech, Inc., Stony Brook, NY, USA) was dissolved in 20 ml of water by stirring vigorously overnight. To obtain ca. 5% modification of carboxyl groups (0.0125 mmol), 18.6 mg of biotin-LC-hydrazide (Pierce, Rockford, IL, USA) dissolved in 180 μl dimethylsulfoxide (DMSO) was added, followed by 24 mg (0.125 mmol) of 1-[3-(dimethylamino)propyl]-3-ethylcarbodiimide hydrochloride. The bHA was purified by extensive dialysis over several days, alternating between 500 mM NaCl and water [56].

5.4. bHA blot method

PVDF membranes (Bio-Rad) were pre-wetted in MeOH and then 3–5 μl of the protein was added dropwise as the MeOH evaporated. After the membrane absorbed the protein solution, it was immediately immersed in blocking buffer (TBS+1% polyvinyl pyrrolidone (PVP-40) and 1% casein) for 2 h. The mem-

brane was then incubated with 10 μg/ml of bHA in blocking solution for 2 h, washed three times with TBS-T, incubated with 1:4000 dilution of SA–HRP for 40 min, washed, and visualized after a 60 s incubation with BM chemiluminescent ELISA substrate (Boehringer Mannheim). The membrane was covered with plastic wrap and immediately exposed to X-ray film (X-Omat-AR film, Kodak). The signal was quantified with a computer-controlled scanner (UMAX 1200S), and the digitized signal was analyzed using NIH Image.

5.5. Construction of the peptide libraries

Two eight-amino acid one-bead, one-peptide libraries were constructed [57]. Library **R** was a completely random library in which only cysteine was omitted during synthesis. Library **B** had an alternating acidic pattern, XZXZXZXZ, with X = any residue except Cys, Arg, or Lys, and Z = D-Asp, L-Asp, D-Glu, or L-Glu. Thus, Tentagel S NH_2 beads (Rappe Polymere GmbH, Tübingen, Germany) are 80–100 μm in diameter with 0.3 mmol reactive amine/g dry weight [57,58]. A typical starting sample size was six million beads, which were incubated with 9-fluorenylmethoxycarbonyl (Fmoc)-protected amino acids whose free carboxyls were activated with 1-hydroxybenzotriazole and *o*-benzotriazol-1-yl-*N*,*N*,*N*′,*N*′-tetramethyluronium hexafluorophosphate (Advanced Chemtech, Louisville, KY, USA). The reaction proceeded in dimethylformamide (DMF) and the beads were purified at each step by washing with DMF. The Fmoc-protected amine was deprotected using 20% piperidine in DMF and quantitative analysis determined the amount of available amine. To ensure a completely random library for Library **R**, the following strategy was used. The entire batch of beads was split into 19 equal pools, each in a separate plastic column. Each batch was allowed to react with a single variety of Fmoc amino acid followed by a DMF wash. All beads were then combined, mixed, and then separated again into 19 new pools, and the process was repeated eight times. This method ensures the presence of a random population of peptides, while only one species is attached per bead. An analogous split-pool-split procedure was performed for Library **B**, alternating between a four-pool split and a 17-pool split.

5.6. Bead screening

Beads (2 ml, approximately 2×10^5 beads) from Library **B** or Library **R** were placed in a 5-ml plastic column (Bio-Rad) and pretreated by washing with decreasing concentrations of DMF in TBS and finally with TBS containing 0.1% PVP-40. Next, 1 ng/ml of GST–RHAMM(518–580) was incubated with the beads for 1 h at room temperature on an orbital shaker. The beads were washed with 20 column volumes of buffer, and incubated with a 1:5000 dilution of anti-GST. This washing was repeated, followed by incubation with a 1:10 000 dilution of anti-goat IgG alkaline phosphatase. After extensive washing, the beads were then incubated with 0.27 mM 5-bromo-4-chloro-3-indolyl phosphate in detection buffer (TBS+2 mM $MgCl_2$). The positive beads turned blue within 10–30 min, and were then sorted under 100× magnification using a syringe fitted with a 10-μl pipette tip. The beads were stripped of bound protein and color by washing with 6 M guanidinium hydrochloride, pH 2.5, followed by three washes with DMF. This screening process was repeated three times, with the total number of beads decreasing after each successive screen. The final screen included a pre-incubation step with 1 mg/ml digested HA as competitor, such that beads that did not turn blue in the final screen were candidates for binding to the HABD of RHAMM.

Peptides on beads were sequenced by placing a single bead on a filter in the same manner that a polypeptide in solution would be immobilized. Sequencing was accomplished using Edman degradation chemistry on an Applied Biosystems Model 477A Gas Phase Peptide Sequencer. A single 'white' bead from the first screening was selected as a negative control, designated peptide **NB**, and its sequence was determined to be IDSDWEGE.

5.7. Pepspots® analysis of biased library results to determine chirality of peptides

Each of the 16 possible diastereomers for four positive Library **B** peptides was synthesized in spots immobilized on cellulose (Pepspots®, Jerini Biotools, Wilmington, NC, USA). Four diastereomers of the negative control peptide **NB** (IDSDWEGE) were also synthesized. The amount of immobilized peptide is reported to be 3–5 nmol on the membrane as a 2-mm dot.

Binding to the Pepspots® was detected by incubation of the blocked (TBS+0.1% casein) membrane with 50 μg/ml GST–RHAMM(518–580) in blocking buffer. After washing, the bound protein was semi-dry electrotransferred from the cellulose membrane onto a PVDF membrane using the Phast (Pharmacia) system. A system of three buffers recommended by Jerini Biotools was used in this transfer: cathode buffer (25 mM Tris, 40 mM 6-aminohexanoic acid, 0.01% sodium dodecyl sulfate and 20% methanol); anode buffer I (30 mM Tris base, 20% methanol); and anode buffer II (300 mM Tris base, 20% methanol). Filter paper squares were soaked in these buffers, three sets for each membrane to be transferred. First, the anode buffer I-soaked filter papers were placed on the anode, followed by the anode buffer II-soaked membranes; the two membranes were arranged with the PVDF membrane on the anode side of the cellulose membrane. The sandwich was completed with the cathode buffer-soaked filter papers. The cathode was placed on top of the sandwich and the transfer was performed at 0.8 mA/cm^2 of membrane for 40 min at 4°C.

The PVDF membrane with the blotted GST–RHAMM(518–580) was blocked and incubated with a 1:5000 dilution of anti-GST, followed by a 1:10 000 dilution of anti-goat antibody–HRP. To detect bound material, a chemiluminescence detection kit (Boehringer Mannheim) was used followed by exposure to film. The developed film was scanned and quantified as above. Each experiment was repeated several times with different GST–RHAMM(518–580) concentrations; increased GST–RHAMM(518–580) concentrations resulted in increased background and non-specific binding.

5.8. Synthesis of labeled peptides for binding assays

Peptides were synthesized using conventional Fmoc chemistry on an Applied Biosystems Model 431A Peptide Synthesizer. The synthesized peptides were split into two batches. The first batch remained unlabeled, while a second batch was carried through an additional synthetic cycle to add an N-terminal Cys. All cleaved peptides were characterized by matrix-assisted laser desorption ionization-time of flight and purified on high performance liquid chromatography (HPLC) prior to use.

Either N^{α}-(3-maleimidylpropionyl)biocytin or fluorescein-5-maleimide (Molecular Probes, Eugene, OR, USA) was linked to the free thiol of the N-terminal Cys, using a three times molar excess of maleimide and ca. 1 mg of peptide. The maleimide probe was dissolved in DMSO to 10 mg/ml and the peptide was dissolved in 20 mM Tris, pH 7.0 to 1 mg/ml in a microfuge tube. The Cys-containing peptides were handled in degassed reaction buffers and lyophilized from trifluoroacetic acid solutions to maintain the free thiol. After mixing the peptide and maleimide reagents, precipitation occurred in some cases; for those mixtures, the reaction was centrifuged at $16\,000 \times g$ for 2 min, and the reaction supernatant was removed and recombined with the DMSO-redissolved precipitate. After shaking for 12 h at room temperature, the conjugated peptides were purified by HPLC.

5.9. Preparation of low molecular weight HA

Bacterially expressed HA (700–1200 kDa) was dissolved overnight in 50 mM sodium acetate buffer (pH 6.0) to give a 4 mg/ml solution. Ten units of testicular HAse (Sigma) per mg HA were added to the solution and the reaction was shaken for 12 h at 37°C. An additional aliquot of HAse was added and the solution was again incubated at 37°C for 12 h. This material was boiled for 5 min to inactivate any remaining HAse, and particulate matter was removed by centrifugation. The molecular weight was analyzed using gel permeation chromatography (Waters), which showed a distribution of molecular sizes from 4 to 40 kDa. This material was employed in the binding assays.

5.10. Solid-phase binding assay

GST–RHAMM(518–580) was immobilized in a 96-well plate (Greiner GmbH) and either bHA or biotinylated peptides were added. Bound probes were detected using SA–HRP and the colorimetric HRP substrate 3,3′,5′,5-tetramethylbenzidine (TMB). Thus, 50 μl of 0.5 mg/ml GST–RHAMM(518–580) in 50 mM Tris (pH 8.0) was incubated in each well for 1 h at 4°C with shaking. The wells were washed with TBS-T (20 mM Tris, 130 mM NaCl, pH 7.6, 0.1% Tween) three times, and then blocked with TBS-T–PVP-40 (TBS-T+0.1% PVP-40) for 2 h at 4°C. Dilutions of biotinylated probe (either HA or peptide) were added to each well in 50 μl TBS-T–PVP-40. After incubation for 45 min, wells were washed with TBS-T and bound biotinylated probes were detected using 50 μl 0.5 μg/ml SA–HRP (40 min, room temperature). After three washes, 50 μl TMB was added and color was detected after 10 min using a Perkin Elmer HTS-7000 microplate reader with the absorbance filter set at 360 nm. Experiments were performed in triplicate, and background was measured using a biotinylated probe that was added to blocked wells lacking GST–RHAMM(518–580). Control experiments included measuring binding with the negative control peptide **NB**.

Alternatively, this experiment was performed using fluorescein-labeled peptides rather than biotinylated peptides. In this case, after the incubation step with fluorescein-labeled probes, the plate was washed three times with TBS-T and then 50 μl TBS was added to each well. The plate was then read on the microplate reader using 485 nm excitation and 535 nm emission filters. The gain was set to optimal and 50 flashes were used to improve sensitivity.

5.11. FP binding assay

Purified GST–RHAMM(518–580) was prepared at a stock concentration of 1.3 mg/ml (40 μM), and the initial concentration of fluorescent peptide was 0.1 μM. Thus, 200 μl of each dilution of GST–RHAMM(518–580) was added to the wells of a low-bind 96-well plate with black sides and a clear bottom (Corning Costar). For each set of experiments, the fluorescein-labeled probe concentration was kept constant, while the concentration of protein was incremented. Data were collected using a Polarion (Tecan Inc.) microplate spectrofluorimeter equipped with a 485 nm excitation filter and a 585 nm emission filter. Fifty flashes were used to achieve optimal sensitivity, and free fluorescein was used as a standard at a value of 20 mP (millipolarization units). To generate a binding isotherm, a plate was prepared with triplicates of each concentration, serial dilutions of GST–RHAMM(518–580) optimally covering the range from 20-fold below the K_D to approximately 100-fold above the K_D. Identical aliquots of fluorescein–peptide were added to each well, the solutions were thoroughly mixed, the plate was incubated until equilibration was reached, and then the fluorescence anisotropy was measured. The binding data, mP values, and receptor concentrations were used to calculate the binding constants. This assay is most useful for probes that bind with K_D values < 1 μM, which constitutes a practical limit of protein concentrations needed to generate the isotherm.

FP data were analyzed as described [43,59] to measure the amount of ligand bound by measurement of the anisotropy of the complex. The total change in polarization is calculated as $\Delta mP = mP_{max} - mP_{min}$. The bound ligand at each concentration is calculated as $B_T = [(mP - mP_{min})(\text{total tracer concentration})]/\Delta mP$. Assuming 1:1 stoichiometry, $B_T = R_{bound}$, and free [HABD] can be calculated as $R_{free} = R_{tot} - R_{bound}$. Scatchard analysis by plotting R_{bound}/R_{free} vs. R_{bound} led to a best-fit line with a slope equal to the negative reciprocal of the K_D [43].

5.12. Competition experiments using a fluorescence-based solid-phase binding assay

Competition experiments were performed as outlined above except the blocking buffer included 1 mg/ml competitor. The wells were pre-incubated with competitor, and the biotinylated or fluorescein-labeled probe was added together with competitor. Digested HA was used for competition. Heparin, CS-A, and CS-C were dissolved in H_2O to 10 mg/ml, and were diluted to 1 mg/ml in TBS-T–PVP-40 in the competition experiments.

Acknowledgements

This work was supported by grants to G.D.P. from the US Department of Defense, the State of Utah Centers of Excellence Program, and The University of Utah (UT, USA), and by a grant to E.A.T. from the National Cancer Institute of Canada. We thank Dr. J.T. Elliott (The University at Stony Brook, USB) and Professor R. El Magrahbi (USB) for biophysical advice, Mr. R. Gerhart (UT, USA) for bead-picking, and Dr. R.W. Schackmann (UT, USA) for peptide sequencing and synthesis.

References

[1] J.R.E. Fraser, T.C. Laurent, U.B.G. Laurent, Hyaluronan: Its nature, distribution, functions and turnover, J. Intern. Med. 242 (1997) 27–33.

[2] B.P. Toole, Hyaluronan in morphogenesis, J. Intern. Med. 242 (1997) 35–40.

[3] O. Oksala, T. Salo, R. Tammi, L. Hakkinen, M. Jalkanen, P. Inki, H. Larjava, Expression of proteoglycans and hyaluronan during wound healing, J. Histochem. Cytochem. 43 (1995) 125–135.

[4] J. Entwistle, C.L. Hall, E.A. Turley, HA receptors: regulators of signalling to the cytoskeleton, J. Cell. Biochem. 61 (1996) 569–577.

[5] L. Sherman, J. Sleeman, P. Herrlich, H. Ponta, Hyaluronate receptors: key players in growth, differentiation, migration and tumor progression, Curr. Opin. Cell Biol. 6 (1994) 726–733.

[6] E.A. Turley, R. Harrison, www.glycoforum.gr.jp, 1999.

[7] S. Zhang, M.C. Chang, D. Zylka, S. Turley, R. Harrison, E.A. Turley, The hyaluronan receptor RHAMM regulates extracellular-regulated kinase, J. Biol. Chem. 273 (1998) 11342–11348.

[8] C.L. Hall, C. Wang, L.A. Lange, E.A. Turley, Hyaluronan and the hyaluronan receptor RHAMM promote focal adhesion turnover and transient tyrosine kinase activity, J. Cell Biol. 126 (1994) 575–588.

[9] C.L. Hall, L.A. Lange, D.A. Prober, S. Zhang, E.A. Turley, pp60(c-src) is required for cell locomotion regulated by the hyaluronan receptor RHAMM, Oncogene 13 (1996) 2213–2224.

[10] C.L. Hall, B. Yang, X. Yang, S. Zhang, M. Turley, S. Samuel, L.A. Lange, C. Wang, G.D. Curpen, R.C. Savani, E.A. Turley, Overexpression of the hyaluronan receptor RHAMM is transforming and is also required for H-ras transformation, Cell 82 (1995) 19–26.

[11] V. Lokeshwar, M. Selzer, Differences in hyaluronic acid-mediated functions and signaling in arterial, microvessel, and vein-derived human endothelial cells, J. Biol. Chem. 274 (2000) 27641–27649.

[12] Y. Yamada, N. Itano, H. Narimatsu, T. Kudo, S. Hirohashi, A. Ochiai, A. Niimi, M. Ueda, K. Kimata, Receptor for hyaluronan-mediated motility and CD44 expressions in colon cancer assessed by quantitative analysis using real-time reverse transcriptase-polymerase chain reaction, Jpn. J. Cancer Res. 90 (1999) 987–992.

[13] C. Wang, A.D. Thor, D.H. Moore II, Y. Zhao, R. Kerschmann, R. Stern, P.H. Watson, E.A. Turley, The overexpression of RHAMM, a hyaluronan-binding protein that regulates ras signaling, correlates with overexpression of mitogen-activated protein kinase and is a significant parameter in breast cancer progression, Clin. Cancer Res. 4 (1998) 567–576.

[14] V. Assmann, J.F. Marshall, C. Fieber, M. Hofmann, I.R. Hart, The human hyaluronan receptor RHAMM is expressed as an intracellular protein in breast cancer cells, J. Cell Sci. 111 (1998) 1685–1694.

[15] V. Abetamann, H.F. Kern, H.P. Elsasser, Differential expression of the hyaluronan receptors CD44 and RHAMM in human pancreatic cancer cells, Clin. Cancer Res. 2 (1996) 1607–1618.

[16] M. Crainie, A.R. Belch, M.J. Mant, L.M. Pilarski, Overexpression of the receptor for hyaluronan-mediated motility (RHAMM) characterizes the malignant clone in multiple myeloma: identification of three distinct RHAMM variants, Blood 93 (1999) 1684–1696.

[17] K.J. Till, M. Zuzel, J.C. Cawley, The role of hyaluronan and interleukin 8 in the migration of chronic lymphocytic leukemia cells within lymphoreticular tissues, Cancer Res. 59 (1999) 4419–4426.

[18] L.M. Pilarski, E. Pruski, J. Wizniak, D. Paine, K. Seeberger, M.J. Mant, C.B. Brown, A.R. Belch, Potential role for hyaluronan and the hyaluronan receptor RHAMM in mobilization and trafficking of hematopoietic progenitor cells, Blood 93 (1999) 2918–2927.

[19] L. Collis, C. Hall, L. Lange, M. Ziebell, R. Prestwich, E.A. Turley, Rapid hyaluronan uptake is associated with enhanced motility: implications for an intracellular mode of action, FEBS Lett. 440 (1998) 444–449.

[20] V. Assmann, D. Jenkinson, J.F. Marshall, I.R. Hart, The intracellular hyaluronan receptor RHAMM/IHABP interacts with microtubules and actin filaments, J. Cell Sci. 112 (1999) 3943–3954.

[21] B. Yang, L. Zhang, E.A. Turley, Identification of two hyaluronan-binding domains in the hyaluronan receptor RHAMM, J. Biol. Chem. 268 (1993) 8617–8623.

[22] B.H. Yang, B.L. Yang, R.C. Savani, E.A. Turley, Identification of a common hyaluronan binding motif in the hyaluronan binding proteins RHAMM, CD44 and link protein, EMBO J. 13 (1994) 286–296.

[23] A.J. Day, The structure and regulation of hyaluronan-binding proteins, Biochem. Soc. Trans. 27 (1999) 115–121.

[24] B. Yang, C.L. Hall, B.L. Yang, R.C. Savani, E.A. Turley, Identification of a novel heparin binding domain in RHAMM and evidence that it modifies HA mediated locomotion of ras-transformed cells, J. Cell. Biochem. 56 (1994) 455–468.

[25] M. Ziebell, Ph.D. Thesis, The University at Stony Brook, Stony Brook, NY, 2000.

[26] D. Kohda, C.J. Morton, A.A. Parkar, H. Hatanaka, F.M. Inagaki, I.D. Campbell, A.J. Day, Solution structure of the link module: a hyaluronan-binding domain involved in extracellular matrix stability and cell migration, Cell 86 (1996) 767–775.

[27] J. Bajorath, B. Greenfield, S.B. Munro, A.J. Day, A. Aruffo, Identification of CD44 residues important for hyaluronan binding and delineation of the binding site, J. Biol. Chem. 273 (1998) 338–343.

[28] J. Entwistle, S.W. Zhang, B.H. Yang, C. Wong, Q. Li, C.L. Hall, M. Mowat, A.H. Greenberg, E.A. Turley, Characterization of the murine gene encoding the hyaluronan receptor RHAMM, Gene 163 (1995) 233–238.

[29] K.S. Lam, Application of combinatorial library methods in cancer research and drug discovery, Anticancer Drug Des. 12 (1997) 145–167.

[30] B.H. Yang, B.L. Yang, P.F. Goetinck, Biotinylated hyaluronic acid as a probe for identifying hyaluronic acid-binding proteins, Anal. Biochem. 228 (1995) 299–306.

[31] K. Hoare, R.C. Savani, C. Wang, B. Yang, E.A. Turley, Identification of hyaluronan binding proteins using a biotinylated hyaluronan probe, Connect. Tissue Res. 30 (1993) 117–126.

[32] J.E. Scott, F. Heatley, Hyaluronan forms specific stable tertiary structures in aqueous solution: a ^{13}C NMR study, Proc. Natl. Acad. Sci. USA 96 (1999) 4850–4855.

[33] J.E. Scott, Secondary structures in hyaluronan solutions: chemical and biological implications, in: C. Foundation (Ed.), The Biology of Hyaluronan, J. Wiley and Sons, Chichester, 1989, pp. 6–20.

[34] J. Kahmann, R. O'Brien, J. Werner, D. Heinegard, J. Ladbury, I. Campbell, A. Day, Localization and characterization of the hyaluronan-binding site on the Link module from human TSG-6, Structure 8 (2000) 763–774.

[35] B. Friguet, A.F. Chaffotte, L. Djavadi-Ohaniance, M.E. Goldberg, Measurements of the true affinity constant in solution of antigen–antibody complexes by enzyme-linked immunosorbent assay, J. Immunol. Methods 77 (1985) 305–319.

[36] E. Gold, An interaction of albumin with hyaluronic acid and chondroitin sulfate, Biopolymers 19 (1982) 1407–1414.

[37] S. Xu, J. Yamanaka, S. Sato, I. Miyama, M. Yonese, Characteristics of complexes composed of sodium hyaluronate and bovine serum albumin, Chem. Pharm. Bull. 48 (2000) 779–783.

[38] T. Fujimoto, H. Kawashima, T. Tanaka, M. Hirose, N. Toyama-Sorimachi, Y. Matsuzawa, M. Miyasaka, CD44 binds a chondroitin sulfate proteoglycan, aggrecan, Int. Immunol. 13 (2001) 359–366.

[39] H. Kawashima, M. Hirose, J. Hirose, D. Nagakubo, A. Plaas, M. Miyasaka, Binding of a large chondroitin sulfate/dermatan sulfate proteoglycan, versican, to L-selectin, P-selectin, and CD44, J. Biol. Chem. 275 (2000) 35448–35456.

[40] C. Termeer, J. Hennies, U. Voith, T. Ahren, J. Weiss, P. Prehm, J. Simon, Oligosaccharides of hyaluronan are potent activators of dendritic cells, J. Immunol. 165 (2000) 1863–1870.

[41] W.J. Checovich, R.E. Bolger, T. Burke, Fluorescence polarization: a new tool for cell and molecular biology, Nature 375 (1995) 254–256.
[42] A. Wei, J. Herron, Detection of HCG–anti-HCG interactions by fluorescence polarization, Anal. Chem. 65 (1993) 3372–3377.
[43] B.A. Lynch, K.A. Loiacono, C.L. Tiong, S.E. Adams, I.A. MacNeil, A fluorescence polarization based Src–SH2 binding assay, Anal. Biochem. 247 (1997) 77–82.
[44] T.H. Lee, H.G. Wisniewski, J. Vilcek, A novel secretory tumor necrosis factor-inducible protein (TSG-6) is a member of the family of hyaluronate binding proteins, closely related to the adhesion receptor CD44, J. Cell Biol. 116 (1992) 545–557.
[45] W.T. Winter, S. Arnott, Hyaluronic acid: The role of divalent cations in conformation and packing, J. Mol. Biol. 117 (1977) 761–784.
[46] C. Wang, J. Entwistle, G.P. Hou, Q.A. Li, E.A. Turley, The characterization of a human RHAMM cDNA: conservation of the hyaluronan-binding domains, Gene 174 (1996) 299–306.
[47] S. Zhang, M. Ziebell, W.-F. Cheung, J. Lu, A. Haddad, D. Litchfield, N. Ahn, T. Cruz, G. Prestwich, E. Turley, Intracellular RHAMM is an erk1 binding protein and removal of its N-terminal sequence is required for activation of erk1, Mol. Biol. Cell (2000) submitted.
[48] T. Fukumoto, N. Torigoe, S. Kawabata, M. Murakami, T. Uede, T. Nishi, Y. Ito, K. Sugimura, Peptide mimics of the CTLA4-binding domain stimulate T-cell proliferation, Nat. Biotechnol. 16 (1998) 267–270.
[49] G.M. Dubowchik, M.A. Walker, Receptor-mediated and enzyme-dependent targeting of cytotoxic anticancer drugs, Pharmacol. Ther. 83 (1999) 67–123.
[50] Y. Luo, M.R. Ziebell, G.D. Prestwich, A hyaluronic acid–Taxol antitumor bioconjugate targeted to cancer cells, Biomacromolecules 1 (2000) 208–218.
[51] K.P. Vercruysse, G.D. Prestwich, Hyaluronate derivatives in drug delivery, Crit. Rev. Ther. Drug Carr. Syst. 15 (1998) 513–555.
[52] P.A.G. McCourt, B.H. Smedsrod, J. Melkko, S. Johansson, Characterization of a hyaluronan receptor on rat sinusoidal liver endothelial cells and its functional relationship to scavenger receptors, Hepatology 30 (1999) 1276–1286.
[53] J. Sambrook, E.F. Fritsch, T. Maniatis, Molecular Cloning, A Laboratory Manual, 2nd edn., Cold Spring Harbor Laboratory Press, Plainview, NY, 1989.
[54] T. Pouyani, G.D. Prestwich, Biotinylated hyaluronic acid: a new tool for probing hyaluronate–receptor interactions, Bioconjug. Chem. 5 (1994) 370–372.
[55] Q. Yu, B.P. Toole, Biotinylated hyaluronan as a probe for detection of binding proteins in cells and tissues, Biotechniques 19 (1995) 122–125.
[56] Y. Luo, G.D. Prestwich, Synthesis and selective cytotoxicity of a hyaluronic acid–antitumor bioconjugate, Bioconjug. Chem. 10 (1999) 755–763.
[57] K.S. Lam, M. Lebl, Selectide technology: bead-binding screening, Methods Companion Methods Enzymol. 6 (1994) 372–380.
[58] J. Wu, Q.N. Ma, K.S. Lam, Identifying substrate motifs of protein kinases by a random library approach, Biochemistry 33 (1994) 14825–14833.
[59] W. Dandliker, M. Hsu, J. Levin, B. Rao, Equilibrium and kinetic inhibition assays based upon fluorescence polarization, Methods Enzymol. 74 (1981) 3–28.